

Time stamping in EPRB experiments: application on the test of non-ergodic theories

M.B. Agüero, A.A. Hnilo^a, M.G. Kovalsky, and M.A. Larotonda

Centro de Investigaciones en Laseres y Aplicaciones (CEILAP) (CITEFA-CONICET-UNSAM), CITEFA, J.B. de La Salle 4397, B1603ALO Villa Martelli, Argentina

Received 8 September 2009

Published online 9 October 2009 – © EDP Sciences, Società Italiana di Fisica, Springer-Verlag 2009

Abstract. In Einstein-Podolsky-Rosen-Bohm (EPRB) experiments, the record of the time of detection of each single photon (“time stamping”) provides much more information than the usual record of coincidence rates. It is a preferable technique for several reasons, and it can be realized with accessible means nowadays. As an illustration of its capacities, we show that a certain class of non-ergodic (local realistic) models that violates the Bell’s inequalities, even in ideally perfect setups, is disproved from the examination of time stamped files. This class of models, which has remained untested until now, exploits the finite size of the time window defining the coincidences, and it cannot be disproved by measuring coincidence rates. We use not only our own experimental data, but also the data obtained in the Innsbruck experiment with random variable analyzers.

PACS. 42.50.Xa Optical tests of quantum theory – 03.67.Dd Quantum cryptography and communication security – 03.65.-w Quantum mechanics

1 Introduction

Bell’s inequalities reveal a basic contradiction between quantum mechanics (QM) and the intuitive notions of locality and realism (LR). The experiments aimed to elucidate which of the two conceptions is correct in the Nature have therefore a fundamental interest. Most of the performed experiments are of the EPRB type [1]. In these experiments, for an entangled state of two modes of the electromagnetic field, the rate of coincident photon detections is measured after polarizers oriented at certain angles. Until now, leaving aside a few remaining logical loopholes, the experiments confirm the predictions of QM. However, giving up LR affects our intuitive view of the world so deeply, that the search for alternative explanations is, at some extent, justified.

Non-ergodic theories (NETs) are one of the families of hypothesis that attempt to reconcile the predictions of QM with LR. In general terms, the NETs propose that “ensemble averages” and “run averages” are not equivalent [2]. This means the following: as all QM predictions involve probabilities, an observation must be repeated many times in order to complete a measurement. QM assume that the repetitions are performed on identically prepared copies of the system, being the differences among the observed results a consequence of the intrinsic randomness of the microscopic world. NETs, instead, hypothesize that there is an “interaction or memory” between the consecutive observations, i.e., NETs hypothesize that the observed

results are the consequence of some complex dynamics underlying, that takes into account the system’s history and/or the influence of the environment [3]. The effect of these dynamics, averaged over the period of time the measurement is performed, fits the observable QM predictions without violating LR [4]. Among the models recognized as NETs, the scheme for photon detection proposed by Scalera [5] is particularly simple and powerful. It fits the QM predictions even for an ideal setup with 100% efficiency detectors. This scheme has not been tested until now.

In this paper we present, we believe for the first time, an experimental test of this apparently unbeatable class of NETs. The test is based on the “time stamping” record of the photon detections, i.e., the record not of the average or total rates, but of the time of detection of each photon. In this context, this procedure is also called “time resolved data acquisition” and it is demonstrated to have several advantages [6]. Here we show that it is possible to build up a reliable time stamping setup of acceptable resolution with low cost and simple-to-use devices. In addition, we present the results that can be extracted from the raw data of the more sophisticated experiment performed in Innsbruck [12] with random variable polarizers, which also used time stamping (although for a different reason and purpose).

In the next section we describe the Scalera’s model in its simplest form and the essential characteristics of its further, more complex versions. We then analyze two ways this class of NETs can be disproved by time stamping.

^a e-mail: ahnilo@citefa.gov.ar

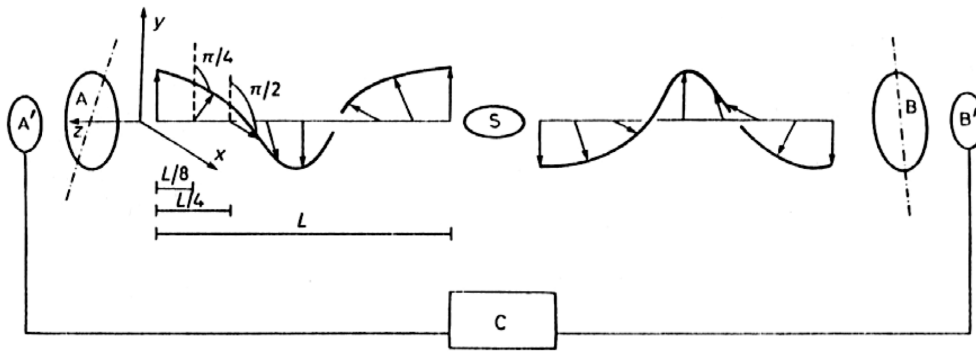


Fig. 1. (from Ref. [5]) Scalera's model in its simplest form. Each "photon" is assumed to be like a ribbon with a helix shape. (A, B) are the polarizers, (A', B') the detectors, C is the coincidence counter, L is the helix step. The little arrows represent the hidden variables of the process.

In the following section, we explain our experimental setup and results, and also the results from the Innsbruck experiment.

2 Scalera's model of photon detection

The model is not claimed to reproduce the physical world although, in the author's words: "*since this class of models has several concomitant similarities with the physical situation, it will be very unpleasant if they do not contain at least a small crumb of truth or some clues leading us towards it*" [9]. Assume that the source emits two correlated beams of light in opposite directions. Each beam consists of a continuous "ribbon", which is helix-shaped and propagates in a direction parallel to its axis (Fig. 1). When a beam reaches a polarizer, the angular orientation of the polarizer (say, α for the station A and β for the station B) is marked on the ribbon. The photon detector placed behind the polarizer integrates the "energy" contained in the ribbon, always starting from a marked direction and ending with the next marked direction. The detector ticks only when two successive marked directions have entered it. It is blind at the initial piece of ribbon arriving before the first marked direction. Therefore, if the axes of the polarizers at A and B are parallel, then the two detectors tick at identical times. If they form an angle $\theta = \alpha - \beta > 0$ instead, then the ribbon at A is marked a distance $\theta L/2\pi$ behind the distance where the ribbon at B is marked (L is the step of the helix, be aware that L is *not* the wavelength, but an arbitrary and unknown distance). In consequence, the detector at A ticks a time $\theta L/(2\pi c)$ after the detector at B, or:

$$t_A - t_B = \theta L/(2\pi c). \quad (1)$$

By definition, the ticks are coincident if:

$$|t_A - t_B| \leq T_w, \quad (2)$$

where T_w is the duration of the time window of the coincidence-counting device. There is a critical angle, θ_c :

$$\theta_c \equiv 2\pi c T_w / L. \quad (3)$$

If the angle between the polarizers is smaller than θ_c , a coincidence is detected. If it is larger, the counts appear uncorrelated. The probability of observing a coincidence, as a function of that angle, has the form of a step-function that can violate the limit imposed by LR (Fig. 2). In particular, if:

$$\pi/8 \leq \theta_c \leq 3\pi/8 \quad (4)$$

the Bell's inequality is strongly violated. In order to see this easily, let's use a simplified expression of the Shimony-Holt-Clauser and Horne correlation parameter S [1]:

$$S = 8[P(\pi/8) - P(3\pi/8)] \quad (5)$$

which coincides with the usual expression in the limit of an infinite number of detected photons. For θ_c fulfilling equation (4) one gets $S = 4$, a value larger than the LR limit of 2 and also larger than the QM-predicted value of $2\sqrt{2}$. As L is a free parameter, it does not matter how small T_w can be, it is always possible to make the critical angle θ_c to take any desired value and to violate LR. By introducing some randomness and adjusting some details [9] the Scalera's model fits the sinusoidal probability functions (and the exact value of S) predicted by QM, even for a setup with two-exit polarizers.

Notarrigo independently presented a more complex scheme, based on two separate subsystems of $M + 2$ classical transverse oscillators coupled by linear interactions between nearest neighbors only [10]. The polarizers were represented as constraints of the oscillation to a direction in the transversal plane. The detectors gave a "count" every time a given dynamical variable of the mechanical system crossed an assigned threshold with positive slope. This model was complex enough to be accessible only through computer simulations. It was obtained that the times of photon detection were practically random. Also, that the sinusoidal shape of the QM-predicted probability functions was well approximated after a convenient choosing of the dynamical variable, a tuning of the simulation's parameters, and M sufficiently large ($M = 20$ to 100, which was the maximum number explored). Finally, it was found that this model converged to the Scalera's one for the particular case $M = 0$ (a single oscillator for each side of the setup) [10]. Leaving aside the details, both models are considered to belong to the same class of NETs.

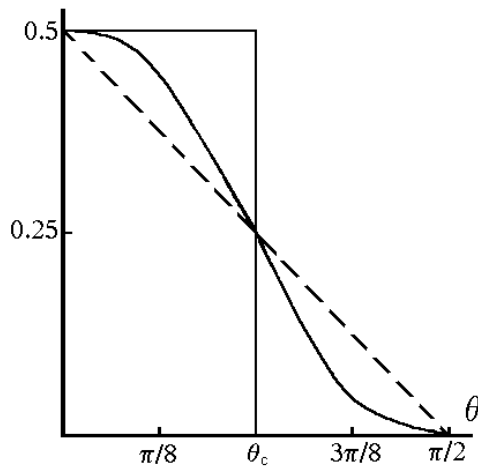


Fig. 2. Probability of coincidence as a function of the angle between the polarizers, $\theta \equiv \alpha - \beta$. The dotted line corresponds to the limit imposed by LR: no curve can be above this line in the interval $(0, \pi/4)$ and below it in $(\pi/4, \pi/2)$. The sinusoidal curve is the QM prediction for the fully symmetrical Bell state $|\Phi^+\rangle$. The steplike function corresponds to the Scalera’s model with $\theta_c = \pi/4$. Note that it violates the LR limit in a stronger way than QM.

In fact, in this class of NETs not a single photon emitted by the source is lost; all what happens is that its detection is shifted in time. This class of NETs holds even in an ideal setup with 100% efficient optics and detectors, and with fast, random variation of the orientation of the polarizers. In spite of these apparently unbeatable features, a test can be performed by “time stamping” in at least two different ways, as we discuss next.

Note that, in a time stamped file, the value of T_w can be varied at will after the experiment has been completed. Any correlation between the values of T_w and those of L and θ is, in consequence, impossible. Let consider first the simplest Scalera’s model. If one chooses a very large value of T_w , long enough so that the detections at A and B always fall inside the coincidence window, then $P(\theta) = 1/2$ for all θ and, from equation (5), $S = 0$. If one chooses a very short value of T_w instead, $P(\theta) = 0$ for all $\theta \neq 0$ and $S = 0$ again. At intermediate values of T_w the value of S can be made to fit the QM predictions. The two drops in the value of S occur at the limits given by the double inequality equation (4). Hence, if S falls to zero at T_w' because $3\pi/8 = 2\pi cT_w'/L$ (rhs of Eq. (4)), it must fall to zero again at $T_w'/3$ (lhs of Eq. (4)). The maximum value of S is reached between these two drops. In the more complex versions of this class of NETs the transitions are smooth instead of sharp, but these features remain the same.

To see if these features provide a condition able to discriminate this class of NETs from QM, let’s see what happens with $S = S(T_w)$ according to QM. In this case, one assumes that the data files are composed of:

- 1) “pairwise coincidences”, for which $t_A - t_B$ is not strictly equal to zero because of instrumental imperfections (thus $t_A - t_B$ is small and has just some statistical spread); and

- 2) “noise”, that produces well separated in time, uncorrelated counts in files A and B.

A large T_w includes as coincidences a large number of “noisy” counts, and therefore the measured value of S is low. If T_w is decreased, the noisy counts are filtered out and the value of S increases. But, decreasing T_w also decreases the total number of coincidences, therefore increasing the statistical fluctuations and the error bars. If the files are too noisy and S drops at a relatively small value of T_w' , then $T_w'/3$ may fall into the large error bars region and the two curves (the QM prediction and the NET prediction) may remain unresolved. Also, it may happen $T_w'/3$ to fall below the minimum resolution time of the setup. In consequence, it is not immediate that an experiment can discriminate QM from this class of NETs in this way (i.e., the $S(T_w)$ curve).

A second, general way to test this class of NETs is to measure the average time separation between detections at stations A and B, $\langle t_A - t_B \rangle$, for each value of the angle θ between the polarizers. Note that, leaving aside the details, this class of NETs changes the probability of coincidence by displacing the detections in time. A smaller probability of coincidence $P(\theta)$ corresponds to a larger value of $|t_A - t_B|$. Therefore, if this class of NETs were true, $\langle t_A - t_B \rangle$ should be some appropriate function of θ [9,10]. Of course, QM do not predict that any such function exists. The hypothetical correlation between the values of $\langle t_A - t_B \rangle$ and θ cannot be observed in the coincidence rates but, if the resolution time suffices, it can be easily extracted from a time stamped file.

In summary, whether this class of NETs can be discriminated from QM by time stamping, or not, depends on the time resolution and the level of noise of the setup. In no case it can be discriminated by measuring average rates only. In the next section we present the experimental results.

3 Experiments with time stamping

Our setup uses parametric down conversion fluorescence in a double-crystal BBO-I [11], pumped by a 50 mW CW diode laser at 405 nm. The nearly degenerate frequency-down converted photons at 810 nm are detected with silicon avalanche photodiodes coupled through multimode optical fibers (core 100 μm , N.A. 0.29). Cube polarizers, AR coated at 810 nm, are inserted before the focusing optics. They are fixed during a run of data recording.

The photon detection modules provide TTL pulses with duration of 30 ns (dark rate $< 250 \text{ s}^{-1}$). These pulses are processed and recorded with a NI 6602 PCI counter timer device. This is a card to be inserted into a PC slot and programmable in LabView. It provides up to three fast output channels (we used only two here) that can be transferred to the RAM of the PC with a time resolution of 12.5 ns and excellent stability. Even though this resolution is inferior to the one achieved in more sophisticated time stamped setups (see below), this approach turns out to be an acceptable solution to the cost-benefit balance for our purposes here.

By appropriate spatial and spectral filtering and phase compensation [11] the fully symmetrical Bell state $|\Phi^+\rangle$ is produced. Using interferential filters (10 nm width) after the polarizers, typical rates are 500 Hz for single counts, 30 Hz ($\theta = 0^\circ$) and 0.3 Hz ($\theta = 90^\circ$) for coincidence rates, and values of S of 2.71 ± 0.03 , therefore violating LR for several tens of standard deviations.

After a set of experiments is completed (each set including usually 20–30 runs) we get two lists of times of detection for each run, one for A and the other for B. The first task then is to plot a histogram of the total number of coincidences as a function of the relative delay between the lists in order to find its optimal value [7] and to measure the actual time resolution. In an ideal setup the optimal delay is zero and the clock defines the resolution, but experimental imperfections (as, say, a different time response of the detectors and the dispersion of the electronic signals) may modify the ideal values. We find that the delay is effectively zero for most of our files and that the width of all the histograms (i.e., the real resolution) is practically 12.5 ns. The specific set of data we use for our study is made of one file for each station (A and B) for the 16 usual different orientations of the polarizers. There are, in consequence, 32 files in the set. Each file lasts 161 s of real time, and has a number of single detections near 80 000. The number of coincidences (delay = 0, $T_w = 12.5$ ns) goes from 4652 ($\theta = 0^\circ$ file) to 68 ($\theta = 90^\circ$ file, accidental coincidences not subtracted). For this set, we compute S for different values of T_w (Fig. 3). As expected, S falls slowly for increasing T_w . The “drop point” T'_w is therefore not sharply defined. One can take one of two criteria:

- 1) T'_w is the value of T_w at which $S = 2$ (the LR limit);
- 2) T'_w is at the elbow of the curve.

In the first case $T'_w \approx 10 \mu\text{s}$ and a second drop should be observed at $T'_w/3 \approx 3 \mu\text{s}$. In the second case $T'_w \approx 2 \mu\text{s}$ and the second drop should occur at about 700 ns. But, both at 3 μs and 700 ns the curve is flat and the error remains small (± 0.03), leaving not space to hide a drop in the value of S . On the contrary, the curve remains flat and well defined at $S \approx 2.7$ down to the system’s resolution time, in full agreement with the QM predictions.

Our experiment is not the only one with time stamping. The one performed in Innsbruck in 1998 [12] used time stamping with an accuracy of 0.5 ns and the additional features of the very large separation between the A and B stations (355 m) and, most interesting of all, with polarizers whose orientation was varied at random during the “time of flight” of the photons from the source to the stations. We repeat the calculus of $S = S(T_w)$ with its *longdist35* file (this file was chosen to be publicly available in the web [12]). The curve is almost identical to ours (Fig. 3). The main difference is that it drops at a smaller value of T_w . This is the natural consequence of the higher rate of single counts (≈ 35 KHz), because a significant number of “noisy” counts, sufficient to deteriorate the value of S , accumulate within a smaller time window. If the $S = 2$ criterion is taken, $T'_w \approx 250$ ns and a drop should be observed also at $T'_w/3 \approx 85$ ns. If the

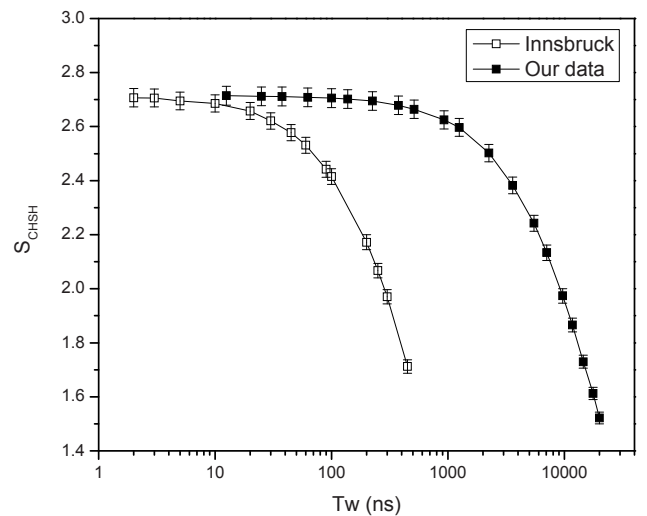


Fig. 3. The correlation parameter S as a function of the time window T_w , experimental results. Error bars are indicated. Note the horizontal logarithmic scale. Full squares: from our data (fixed polarizers) delay = 0. Open squares: from the Innsbruck experiment (varying polarizers) file *longdist35**, delay = 4.5 ns.

elbow-of-the-curve criterion is taken instead, $T'_w \approx 90$ ns and the other drop should occur at about 30 ns. But, once again, the curve is flat both at 85 and 30 ns and it remains so down to the resolution time, being the error everywhere small. The class of NETs under study is in consequence disproved, *also* in the case of random varying polarizers. Nevertheless, a warning is in order regarding the files of the Innsbruck experiment. If T_w is large, the results may become ambiguous. This will be clear a few lines below.

As a further test, we check whether there exists some correlation between the average time separation in the coincident detections at A and B, $\langle t_A - t_B \rangle$, and the angle θ of the polarizers (in Sect. 2, this is named the “second way” to disprove this class of NETs). No shift with θ in the value of $\langle t_A - t_B \rangle$ is found in our data. All the coincidences, for all the 16 different polarizers’ orientations, are in the same position of the clock.

The same calculation with the Innsbruck files poses a problem, for, depending on the value of T_w and the delay between the A and B lists, a single count can produce a coincidence into a certain subset (which corresponds to a given orientation of the polarizers), into another different subset, or not to produce a coincidence at all. We find that the safest way to check whether there is a variation of $\langle t_A - t_B \rangle$ with θ , or not, is by plotting the 16 individual histograms or distributions (one for each orientation of the polarizers) of the number of coincidences as a function of $t_A - t_B$. The main peaks of the 16 distributions have a typical width about 1 ns and fall into an interval 1.6 ns wide, so that they are barely distinguishable. As an illustration see the Figure 4, where the two most separated distributions in the run are displayed (the other 14 fall between them). Besides, there is no apparent trend of variation of $\langle t_A - t_B \rangle$ with θ . A detailed analysis reveals that all the distributions of the form “0j” and “1j” (that

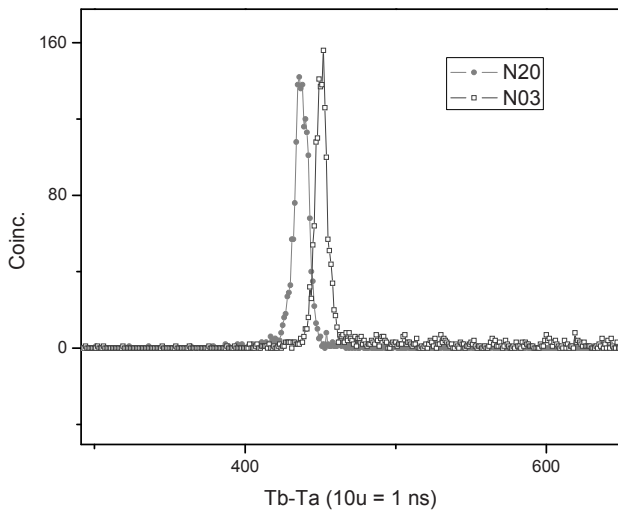


Fig. 4. Distributions of the number of coincidences as a function of $t_B - t_A$, from the Innsbruck experiment. Subset 0–3, in A: high voltage = no, detector=V, in B: high voltage = yes, detector = H, $\theta = \pi/8$, total counts = 1984, peak at 45.2 ns, FWHM = 0.9 ns. Subset 2–0, in A: high voltage = no, detector = H, in B: high voltage = no, detector=V, $\theta = -\pi/8$, total counts = 1801, peak at 43.6 ns, FWHM = 1 ns. File *longdist35**, $T_w = 45$ ns, delay = 4.5 ns.

is, the ones corresponding to a specific detector firing in the A station) are delayed ≈ 1 ns regardless the value of θ . We conclude that the observed shift (which is, anyway, almost negligible) is an artifact caused by a detector with a slower response time, and not the effect predicted by the NETs under study.

It is worth noting that some of these distributions (the N03 in Fig. 4, for example) have many coincidences outside the main peak. Some of them even display well defined secondary peaks, either at the left or at the right of the main peak, and at distances as large as 25 ns. They may lead to confusing results if $\langle t_A - t_B \rangle$ is blindly calculated, instead of obtained from the profiles. The cause of this anomaly is not clear. A plausible cause is a drift between the clocks at stations A and B [13]. This hypothesis is supported by the fact that our setup, which uses a single clock, is free from this anomaly.

In few words: both our data (with unambiguous subsets, but fixed polarizers) and Innsbruck’s (with varying polarizers, but potentially ambiguous subsets) show a variation of $S = S(T_w)$ in agreement with QM and in observable discrepancy with the predictions of the class of NETs under study. Besides, the predicted correlation between $\langle t_A - t_B \rangle$ and θ is not observed in either experiment. We conclude that the class of NETs under study has been disproved.

4 Summary

“Time stamping” or “time resolved data acquisition” setups are a source of valuable information in EPRB setups. They were shown to improve the capacity of discrimina-

tion of the experiment when the predictability of the orientation of the (random variable) polarizers was taken into account [6]. They also allow testing hypothetical deviations from QM having the form of privileged frequencies of the spectrum of fluctuations [7] or the form of low dimensional dynamics. The latter has an impact of practical importance, because it may open a vulnerable flank in the current schemes of quantum cryptography if some simple cautions are not taken [8]. In this paper, we have shown how the Innsbruck’s experiment, a time stamping setup, still provides valuable information more than 10 years after its realization. We have also built up a time stamping setup of satisfactory performance with accessible means. We have used the two complementary sets of data to disprove a class of non-ergodic theories that is not vulnerable by measuring average rates only, and that had remained untested until now.

We deeply acknowledge the generous collaboration of Prof. Gregor Weihs, who not only provided us with the complete data files of the Innsbruck experiment, but also gently and patiently answered many questions via email. Many thanks also to Pablo Saldanha from the Universidade de Minas Gerais and to Christian Schmiegelow from the Universidad de Buenos Aires, who helped to build up the experimental setup. This work was supported by the contracts PICT04-20596, BID 1728 OC/AR (ANPCyT) and PIP08-2917 (CONICET).

References

1. J. Clauser, A. Shimony, Rep. Prog. Phys. **41**, 1881 (1978)
2. The term “non-ergodic theory” was proposed by V. Buonomano; see e.g. Quantum Mechanics vs. Local Realism (Plenum, New York, 1988)
3. Systems with delay, i.e., described by equations of the type: $dx/dt = f(x(t - \tau))$, evolve in a phase space with infinite degrees of freedom and are able to produce a practically random output, even if the dynamics are strictly deterministic
4. R. Gill (with an Appendix by J. Larsson); Accardi contra Bell (cum mundi): the impossible coupling; [arXiv: quant-ph/0110137](https://arxiv.org/abs/quant-ph/0110137)
5. G.C. Scalera, Lett. Nuov. Cim. **38**, 16 (1983)
6. A. Hnilo, Found. Phys. **21**, 547 (1991)
7. A. Hnilo, A. Peuriot, G. Santiago, Found. Phys. Lett. **15**, 359 (2002)
8. A. Hnilo, M. Kovalsky, G. Santiago, Found. Phys. **37**, 80 (2007)
9. G.C. Scalera, Lett. Nuov. Cim. **40**, 353 (1984)
10. S. Notarrigo, Nuov. Cim. **83**, 173 (1984)
11. P. Kwiat, E. Waks, A. White, I. Appelbaum, P. Eberhard, Phys. Rev. A **60**, R773 (1999)
12. G. Weihs, T. Jennewein, C. Simon, H. Weinfurter, A. Zeilinger, Phys. Rev. Lett. **81**, 5039 (1998); also: G. Weihs, Ph.D. thesis, University of Vienna, 1999; also see reference [8] above
13. G. Weihs, private communication, The drift between clocks would also be the cause of the low dimension dynamics observed in reference [8] above